Front. Phys. 10, 107303 (2015)
DOI 10.1007/s11467-015-0493-x

REVIEW ARTICLE

Recent advances in MXene: Preparation, properties, and applications

Jin-Cheng Lei (雷进程), **Xu Zhang** (张旭), **Zhen Zhou** (周震)†

Tianjin Key Laboratory of Metal and Molecule Based Material Chemistry, Key Laboratory of Advanced Energy Materials Chemistry (Ministry of Education), Computational Centre for Molecular Science, Institute of New Energy Material Chemistry, School of Materials Science and Engineering, Collaborative Innovation Center of Chemical Science and Engineering (Tianjin), Nankai University, Tianjin 300071, China

Corresponding author. E-mail: †zhouzhen@nankai.edu.cn

Received March 12, 2015; accepted April 24, 2015

Owing to the exceptional properties of graphene, intensive studies have been carried out on novel two-dimensional (2D) materials. In the past several years, an elegant exfoliation approach has been used to successfully create a new family of 2D transition metal carbides, nitrides, and carbonitrides, termed MXene, from layered MAX phases. More recently, some unique properties of MXene have been discovered leading to proposals of potential applications. In this review, we summarize the latest progress in development of MXene from both a theoretical and experimental view, with emphasis on the possible applications.

Keywords MXene, exfoliation, graphene, 2D materials, supercapacitors

PACS numbers 73.21.Ac, 73.22.-f, 81.05.Je, 81.07.-b, 88.80.-q

Contents

1 Introduction 1
2 Preparation 2
3 Properties 3
3.1 Structural properties 3
3.2 Electronic properties 4
3.3 Chemical properties 4
4 Potential applications 4
4.1 Lithium-ion batteries 4
4.2 Non-lithium-ion batteries 5
4.3 Supercapacitors 6
4.4 Other applications 7
5 Summary and outlook 8
Acknowledgements 8
References and notes 8

1 Introduction

Since the discovery of graphene and its outstanding properties, two-dimensional (2D) materials have become a major research interest in materials science [1–9]. Recently, a new family of 2D materials has emerged, consisting of transition metal carbides, nitrides, and carbonitrides, also known as MXenes [10, 11]. These novel materials are produced by selectively etching layers of *sp* elements from their corresponding three-dimensional (3D) MAX phases [see Fig. 1(a)]. These so-called MAX phases are layered ternary metal carbides, nitrides, or carbonitrides, with a general formula of $M_{n+1}AX_n$ (n = 1, 2, 3), where M, A, and X represent early *d*-block transition metals, main-group *sp* elements (predominantly IIIA or IVA), and either or both C and N atoms, respectively.

Till date, more than 70 MAX phases have been reported [12], but the established MXene family only includes Ti_3C_2, Ti_2C, $(Ti_{0.5}, Nb_{0.5})_2C$, $(V_{0.5}, Cr_{0.5})_3C_2$, Ti_3CN, Ta_4C_3 [13], Nb_2C, V_2C [14], and Nb_4C_3 [15]. More MXene materials are expected to be exfoliated from the sizeable family of MAX phases in the future. Notably, the outer surfaces of the exfoliated layers are always terminated with F, OH, and/or O groups during the etching process [see Fig. 1(b)]. Henceforth, these terminated MXene species will be referred to as $M_{n+1}X_nT_x$, where T represents the surface groups (F, OH, and/or O) and x is the number of terminations.

Since their discovery, MXenes have been reported to possess exceptional properties. For example, the conductivity of MXenes is comparable to that of multilayered graphene [13]. Density functional theory (DFT) computations have shown that MXene is quite stiff, with in-plane elastic constants exceeding 500 GPa [17]. Khazaei

© Higher Education Press and Springer-Verlag Berlin Heidelberg 2015

Frontiers of Physics

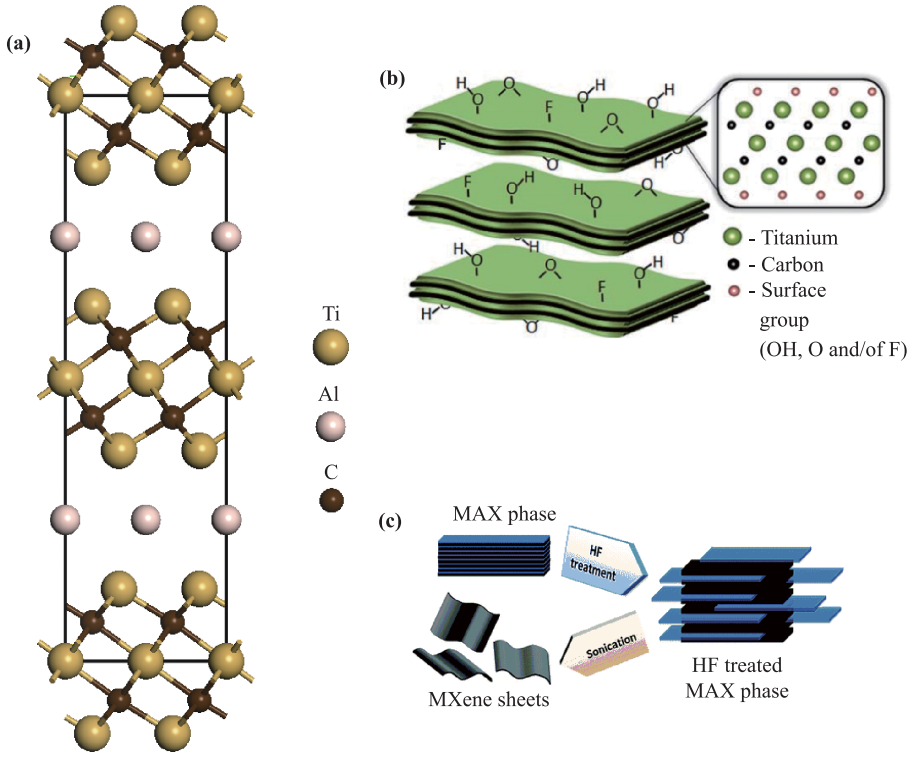


Fig. 1 **(a)** Structure of layered Ti_3AlC_2. **(b)** Terminated MXene. Reprinted with permission from Ref. [16]. Copyright © 2014 Royal Society of Chemistry. **(c)** Schematic showing preparation of MXene from MAX phases. Reproduced with permission from Ref. [13]. Copyright © 2012 American Chemical Society.

et al. found that semiconducting MXenes attain very large Seebeck coefficients at low temperatures [18]. These fascinating properties may lead to important applications and have attracted much attention from researchers in various fields. For example, in energy storage, MXenes are considered to be strong candidates for electrode materials [19, 20]. Xie *et al.* tested MXenes as supporting materials for platinum nanoparticles, achieving an extraordinarily stable catalyst for fuel-cell applications [21]. Wang *et al.* found that MXenes exhibited excellent enzyme immobilization abilities with biocompatibility for redox proteins, which shows promise for applications in electrochemical biosensors [22].

Given the existence of a previous review on MXene [23], here, we will focus on the latest progress in the exploration of MXene, covering both theoretical and experimental studies, with emphasis on the potential applications of this class of materials. We also provide an outlook of future research directions, in the hope that more researchers will explore this new and exciting materials field.

2 Preparation

As mentioned above, MXenes are generally prepared by the selective etching of A layers from their corresponding MAX phases at room temperature, using aqueous HF as the etchant [see Fig. 1(c)]. In the pioneering experiment [10], $Ti_3C_2T_x$ (T = OH and F) was obtained by extracting the weakly bonded Al layers from the Ti_3AlC_2 phase. The reactions of the HF solutions with Ti_3AlC_2 include:

$$Ti_3AlC_2 + 3HF = AlF_3 + 3/2H_2 + Ti_3C_2, \quad (1)$$

$$Ti_3C_2 + 2H_2O = Ti_3C_2\,(OH)_2 + H_2, \quad (2)$$

$$Ti_3C_2 + 2HF = Ti_3C_2F_2 + H_2. \quad (3)$$

Reactions (2) and (3) result in OH and F terminations, respectively. Centrifugation was then performed to separate the solids, which were then washed with deionized water. Without delamination, MXenes possess multilayered structures. To obtain single- or few-layer MXenes, sonication was performed and later replaced by intercalation of dimethyl sulfoxide (DMSO), which proved to be more efficient [24].

This strategy was applied to prepare almost all other MXene sheets from Al-containing MAX phases. Notably, the etching conditions (time and HF concentration) necessary to convert a given MAX phase vary widely, depending on the particle size and temperature. For example, reducing the MAX phase particle size by attrition or ball milling can effectively reduce the necessary etching time and/or HF concentration [14, 25]. In addition, discrepancies in M-Al bond energies for different MAX

phases also require different etching conditions. For example, the larger Ti-Al bond energy in Ti_2AlC compared with the Nb-Al bond energy in Nb_2AlC resulted in extended etching time and increased HF concentration [13, 14]. Hence, appropriate etching conditions are necessary to achieve high yields and complete the conversion of MAX phases into MXenes.

Recently, Halim *et al.* proposed the use of ammonium bifluoride, NH_4HF_2, as an etchant in lieu of the hazardous HF [26]. Its milder nature and concomitant intercalation of cations during the etching process render it more suitable for preparing delaminated MXenes. As the etching and intercalation processes occur simultaneously, it is reasonable to conclude that the following reactions exist:

$$Ti_3AlC_2 + 3NH_4HF_2 = (NH_4)_3AlF_6 + 3/2H_2 + Ti_3C_2 \quad (4)$$

$$Ti_3C_2 + aNH_4HF_2 + bH_2O = (NH_3)_c(NH_4)_dTi_3C_2(OH)_xF_y \quad (5)$$

Because of slower and less vigorous reaction processes, and the intercalation of both NH_3 and NH_4^+, the atomic layers in $Ti_3C_2T_x$ are more uniformly spaced and appear to be glued together.

Ghidiu *et al.* reported a new high-yield method for the simultaneous preparation of many MXene sheets [27]. In this method, $Ti_3C_2T_x$ was prepared by dissolving Ti_3AlC_2 powders in LiF and HCl solutions, then heating the mixture at 40 °C for 45 h, and finally washing the sediment to remove the product and increase the pH. A clay-like paste formed from this processing; this could be rolled to produce flexible, free-standing films with high volumetric capacitance (see the Potential Applications section, below). The process is schematized in Fig. 2(a). The resultant flakes were found to possess larger lateral dimensions with no nanoscale defects, which are frequently observed in HF-etched samples [28] [see Figs. 2(b), (c)]. The lack of defects reflects the milder nature of the LiF + HCl etchant compared with HF. Intriguingly, other combinations of fluoride salts and acids, such as NaF, KF, CsF, tetrabutylammonium fluoride $[(C_4H_9)_4NF]$, and CaF_2 with HCl or H_2SO_4, showed similar etching behaviors. This one-step etching procedure is clearly desirable for future explorations.

3 Properties

3.1 Structural properties

In all real situations, MXene is terminated with surface groups such as F, OH, and O groups after its exfoliation from the MAX phase. O- and/or OH- terminated MXene species were suggested to be the most stable, because F

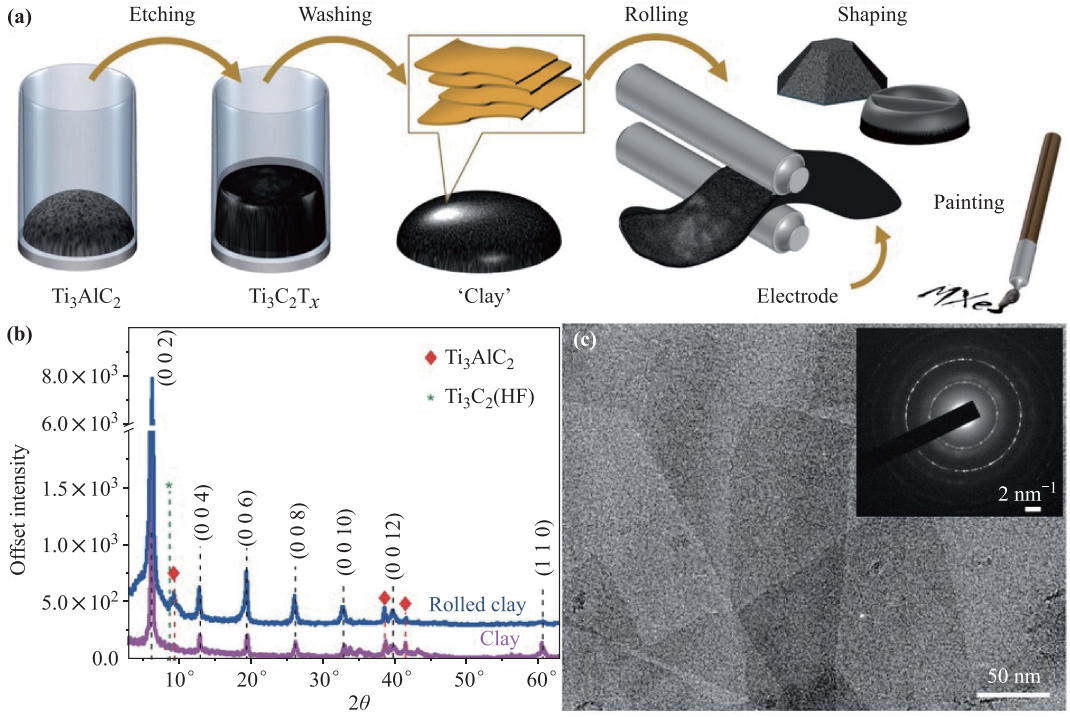


Fig. 2 **(a)** Schematic of preparation of MXene clay. **(b)** X-ray diffraction (XRD) patterns of MXene produced via clay process. **(c)** Transmission electron microscope (TEM) image of several flakes. Reproduced with permission from Ref. [27]. Copyright © 2014 Nature Publishing Group.

terminations will be replaced with OH groups upon rinsing and/or storing in water [29]. Xie *et al.* also found that OH groups can be converted into O terminations through high-temperature treatments and/or metal adsorption processes [29]. In addition, O-terminated MXene can further decompose into bare MXene when in contact with Mg, Ca, Al, or other metals [30].

Modeling has been crucial in understanding MXene's structure [31]. Early predictions indicated that surface groups are more likely to be located above the hollow sites between three neighboring C atoms [32]. However, later studies showed that the locations and orientations of surface groups are more complicated than expected [18]. The exact configurations of surface groups depend on both their species and the MXene's constituent materials. Notably, MXene is usually modeled with uniform terminating species, which is not realistic. Future modeling is necessary to accommodate the coexistence and random adsorption of different surface groups within certain MXenes to more accurately reflect the complicated structure of this material system. Interlayer interactions, such as van der Waals forces and/or hydrogen bonding, should also be taken into account, since multilayer stacking often occurs in reality [33].

3.2 Electronic properties

To this point, the electronic [34], dielectric [35], magnetic [36–39], elastic [40], thermoelectric [41], and optical properties [42] of MXene have been reported via theoretical computations. Few experiments have yet strongly confirmed these predictions. Among these, the electronic properties have been studied most intensively, and we will focus on this topic in this section.

Bare MXene species, such as $Ti_{n+1}X_n$, are known to be metallic in behavior [17]. However, the metallic properties weaken as n values increase, due to the formation of additional Ti-X bonds [42]. In terms of X atoms, titanium nitrides exhibit more metallic properties than titanium carbides do, simply because the N atom possesses one more electron than the C atom. By contrast, terminated MXene sheets are narrow-band-gap semiconductors or metals, depending on the species and orientations of surface groups [32, 43]. To the best of our knowledge, the six terminated MXenes of Ti_2CO_2, Zr_2CO_2, Hf_2CO_2, Sc_2CO_2, Sc_2CF_2, and $Sc_2C(OH)_2$ have band gaps.

However, the band gaps of the first five listed terminated MXene sheets are indirect, while $Sc_2C(OH)_2$ has a small direct band gap [18]. For this reason, it is essential to tune the electronic structure to achieve a direct band gap, especially in the fields of optoelectronics and optics. Lee *et al.* investigated the effects of applied strain on the band gap of Sc_2CO_2 [44], as strain can change interatomic distances and the relative positions of atoms within a material. As the tensile strain increases, the band gap gradually decreases. At a critical tensile strain, the indirect band gap tansfers to a direct one. In addition, they found that Sc_2CO_2 could also experience an indirect-to-direct band gap transition under an external electric field, due to the distinction of the responses of each point in the lowest conduction band to the electric field [45].

Here, we must emphasize the significance of choosing the correct exchange-correlation functionals in DFT computations of band gaps, as different results will be generated based on the chosen functional [46]. Hybrid functionals, such as HSE06, are known to give more accurate results in predicting band gaps, and thus are strongly recommended [38], despite their much higher required computational capacity.

3.3 Chemical properties

Recently, Naguib *et al.* found that $Ti_3C_2T_x$ oxidizes in air, CO_2, or pressurized water [47]. The oxidation was found to form anatase TiO_2 nanocrystals embedded in amorphous carbon sheets (TiO_2-C hybrid structure). Ghassemi *et al.* studied the oxidation mechanism through *in situ* TEM analysis [48]. It was assumed that, during flash oxidation, the top and bottom Ti layers oxidized to form thin anatase nanoparticles; however, during slow oxidation, the top and bottom Ti layers were transformed into sheets of nanocrystalline rutile. As a result, two different TiO_2 phases were produced under the two different oxidation regimes [see Fig. 3].

Similarly, Li *et al.* found that $Ti_3C_2T_x$ could react with O_2 to form TiO_2 in either rutile or anatase phases [49]. However, the produced anatase nanocrystals were evenly distributed on the 2D Ti_3C_2 layers, as distinct from the TiO_2-C hybrid structure. The discrepancy was due to the longer reaction time of approximately 40 min, compared with the < 5 s flash oxidation; the newly formed carbon was unstable. At high temperatures, the anatase phase would transform to rutile. Almost simultaneously, a similar phenomenon was reported for Ti_2CT_x [50]. With heat treatment, anatase TiO_2 formed, before transforming to rutile TiO_2 at higher temperatures.

4 Potential applications

4.1 Lithium-ion batteries

Rechargeable lithium-ion batteries (LIBs) are widely

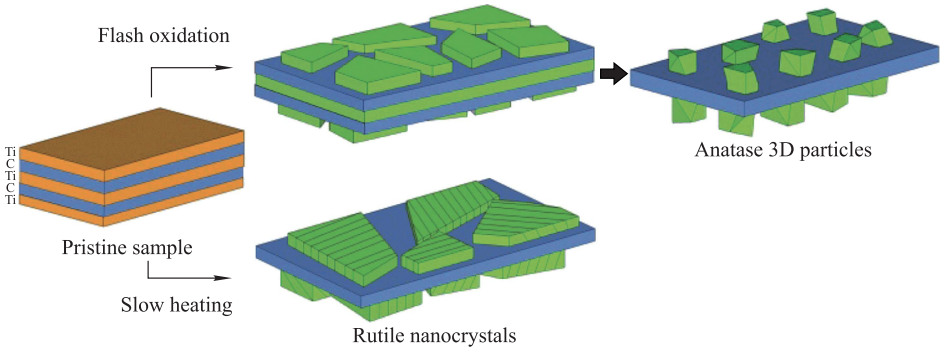


Fig. 3 Schematic of the two oxidation mechanisms. Reproduced with permission from Ref. [48]. Copyright © 2014 Royal Society of Chemistry.

used as energy storage devices. The ideal LIB possesses a high Li storage capacity, good cyclability, and high rate capability, all of which depend on the properties of the LIB's electrode materials. Graphite is the most commonly used anode material, but it suffers from a moderate specific capacity of 372 mAh/g and poor rate capability. Extensive research efforts have explored the development of new anode materials to replace graphite in LIBs.

Soon after their discovery, the feasibility of using MXenes as LIB anode materials was explored [10, 51]. The theoretical Li storage capacity of Ti_3C_2 (in the form of $Ti_3C_2Li_2$) was found to be 320 mAh/g, comparable to that of graphite. Additionally, the predicted diffusion barrier (0.07 eV) for Li on bare Ti_3C_2 was much lower than that of graphite (0.3 eV), which predicted excellent high-rate performances for bare MXene [32]. However, as noted above, all prepared MXene sheets are terminated with surface groups, possibly deteriorating their performance by induced steric hindrance. Compared with other terminated MXene sheets, O-terminated MXene was suggested to possess the highest capacity [29, 30, 52].

Experiments have been performed in addition to computational predictions. Ti_2CT_x [51], V_2CT_x, and Nb_2CT_x [14] were reported to possess reversible capacities of 110 mAh/g, 260 mAh/g, and 170 mAh/g at a rate of 1 C, respectively. However, these values are lower than that of graphite, and thus require improvement. Intercalation and delamination are both known to possibly increase a material's capacity. For example, after DMSO intercalation, $Ti_3C_2T_x$ exhibited a capacity of 123.6 mAh/g at 1 C [53], exceeding that of non-delaminated Ti_3C_2 electrodes (100 mAh/g) [24].

Accordingly, a Ti_3C_2 "paper" was made by filtering the Ti_3C_2 colloidal solution after intercalation with DMSO and dispersing it by sonication [24]. This paper electrode displayed a capacity of 410 mAh/g at 1 C, and maintained a capacity of 110 mAh/g at 36 C after 700 cycles. This high capacity significantly exceeds the maximum theoretical capacity of 320 mAh/g predicted for Ti_3C_2 electrodes. This may be explained by the formation of extra Li layers on the already-lithiated O-terminated MXene, resulting in further enhancement of the capacity [29].

Typically, ion intercalation into battery materials will substantially lower their rate performances, due to diffusion limitations. However, the intercalation of ions into MXene occurs at a very high rate, which poses a paradox. Levi *et al.* resolved this paradox by proposing that cationic insertion occurs so rapidly in MXene that it resembles ion adsorption at the solid-liquid interface; the adsorbed cations are thus electrochemically inserted between the partially swollen layers [54]. Based on this conjecture, two types of cationic adsorption sites (shallow and deep) were believed to be filled with ions and water molecules, which showed a perfect capacitive response over a wide range of charging rates [54].

To further assess the suitability of using MXene as electrode materials, external influences such as strain must be explored, as they may influence MXene's capacity by changing its volume. Via DFT computations, Zhao *et al.* explored the Li adsorption properties of Ti_2C in response to the influences of strain and concentration [55]. Under high strain, the binding energy of Li quickly decreased, but the diffusion barriers showed little change. In addition, neither the binding energy nor the diffusion barriers were visibly influenced by changes in concentration. These computational predictions further demonstrated the high stability and good rate performance of MXene as an electrode material.

4.2 Non-lithium-ion batteries

The large-scale application of LIBs has hidden troubles due to limitations on lithium as a natural resource [56]. Hence, other rechargeable non-lithium-ion batteries (NLIBs), such as Na-, K-, Mg-, Ca-, and Al-ion batteries

have attracted growing attention [30, 52, 57]. Each offers more abundant active material, or doubles the effective capacity as a result of its multi-electron process. As the interactions between these metal ions and C atoms are weak, graphite cannot be used as an anode material in NLIBs. Consequently, the identification of suitable host materials is a critical challenge in NLIB research.

Intriguingly, these metal ions can be intercalated into MXene, which permits the possibility of using MXenes as anode materials for NLIBs [58]. The computed capacities for Na, K, and Ca on Ti_3C_2 are 351.8, 191.8, and 319.8 mAh/g, respectively [57]. Xie *et al.* measured the initial discharge capacities of $Ti_3C_2T_x$ in Na- and K-ion batteries to be 370 and 260 mAh/g, respectively [30]. After 120 cycles, reversible capacities of 80 and 45 mAh/g were retained for Na- and K-ion batteries, respectively. Yang *et al.* investigated the Na storage properties of M_2C-type MXene via DFT computations, finding a theoretical capacity of 190–288 mAh/g [59]. These computational and experimental results clearly demonstrate the feasibility of MXenes as anode materials for NLIBs.

Multivalent-ion batteries generally exhibit higher gravimetric capacities, as their multi-electron redox chemistry prevails over their increased mass. Computations have also predicted that MXene would possess exceptionally high capacities for Mg and Al owing to the multilayer adsorption [30]. Wang *et al.* experimentally observed the formation of double Na-atomic layers in the $Ti_3C_2T_x$ interlayers, confirming the possibility of multilayer adsorption [33]. Future experiments are necessary to test the adsorption of other multivalent ions and the use of MXenes as anode materials for rechargeable NLIBs.

At this juncture, a comprehensive summary is required regarding the influences of surface groups, transition metal species, and intercalation ions on the capacity of MXene anodes. Eames *et al.* performed global screening for high-capacity MXene-based electrode materials [52]. As expected, MXene species containing light transition metals (Sc, V, Ti, or Cr) with non-functionalized or O-terminated surfaces offered the largest gravimetric capacity. In addition, particular attention to multivalent-ion batteries was recommended in future investigations.

4.3 Supercapacitors

Supercapacitors provide alternative energy storage for portable electronics and electric vehicles, but suffer from lower energy densities compared with batteries. Therefore, investigations have focused primarily on improving their energy density per unit volume, i.e., volumetric capacitances. According to their charge-storage mechanisms, supercapacitors can be classified as either electrical double-layer capacitors (EDLCs) or pseudocapacitors. The former are based on the reversible accumulation of ions at the electrode–electrolyte interfaces, while the latter rely on fast and reversible surface redox reactions. Generally, pseudocapacitors possess higher volumetric capacitances, but lack cycling stability.

Owing to their 2D nature, highly defined geometry, and large surface areas, MXenes have been demonstrated as promising electrode materials for supercapacitors. A $Ti_3C_2T_x$ paper electrode was reported to possess an extraordinarily high volumetric capacitance of up to 350 F/cm^3 at 20 mV/s (and 450 F/cm^3 at 2 mV/s) in KOH solutions, with almost no degradation after 10 000 cycles at 1 A/g [58]. These values exceed those of almost all carbon-based EDLCs.

Dall'Agnese *et al.* chemically modified the surface state of $Ti_3C_2T_x$ by intercalation with DMSO, leading to the delamination of $Ti_3C_2T_x$ [60]. The delaminated $Ti_3C_2T_x$ displayed a high intercalation capacitance of 415 F/cm^3 at 5 A/g in an electrolyte of H_2SO_4, and capacitances up to 520 F/cm^3 were recorded at 2 mV/s. As with the paper $Ti_3C_2T_x$ electrode, no significant degradation was observed after 10,000 cycles. This enhanced capacitance can be attributed to the increased surface area and modification of the surface groups to include more oxygen-containing functional groups.

Ghidiu *et al.* utilized rolled films (mentioned in the Preparation section) as supercapacitor electrodes in a H_2SO_4 electrolyte [27]. The electrochemical performances are presented in Fig. 4. A capacitance up to 900 F/cm^3 or 245 F/g was measured, with no measurable loss after 10 000 cycles. This improved electrochemical performance resulted from several factors, including the smaller size of H^+ compared with other intercalating cations, surface redox processes, and improved accessibility to the interlayer space owing to pre-intercalated water.

Additionally, MXene-based composites may also bear great potential as supercapacitor electrodes. Recently, Ling *et al.* reported the properties of a $Ti_3C_2T_x$/polymer composite film, produced by mixing $Ti_3C_2T_x$ and polyvinyl alcohol (PVA) [61]. When used as an electrode, the composite film exhibited an impressive volumetric capacitance as high as 528 F/cm^3 at 2 mV/s and 306 F/cm^3 at 100 mV/s in a KOH electrolyte. Although a slight decrease in capacitance occurred over 10 000 cycles at 5 A/g, the volumetric capacitance of 314 F/cm^3 after 10 000 cycles remained significant, indicating the sufficient cyclic stability of the composite.

Sandwich-like MXene/carbon nanotube (CNT) composite paper electrodes were fabricated through the

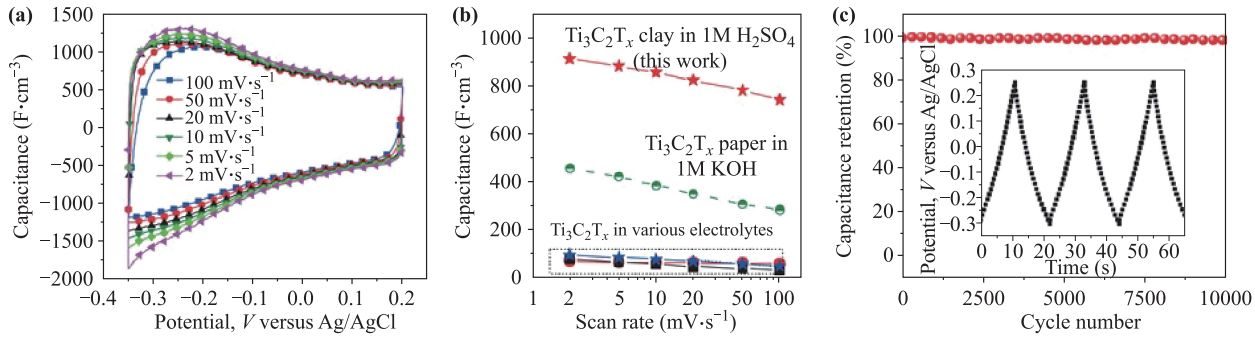


Fig. 4 Electrochemical performances of rolled MXene films. **(a)** Cyclic voltammetry profiles at different scan rates. **(b)** Comparison of rate performances with HF-produced MXene [58]. **(c)** Capacitance retention test. Inset shows galvanostatic cycling data collected at 10 A/g. Reproduced with permission from Ref. [27]. Copyright © 2014 Nature Publishing Group.

alternating filtration of MXene and CNT dispersions [62]. A volumetric capacitance around 345 F/cm^3 at 5 A/g was achieved for $Ti_3C_2T_x$/single-walled CNT paper with no degradation observed after 10 000 cycles. In contrast, although a lower volumetric capacitance of 300 F/cm^3 was yielded at 10 A/g for $Ti_3C_2T_x$/multi-walled CNT paper, this value increased to approximately 350 F/cm^3 after 10 000 cycles, which may have resulted from the improved accessibility of slit pores. Notably, these paper electrodes were tested in an electrolyte of 1 M $MgSO_4$ aqueous solution, which has a rather low conductivity. Thus, the electrode performances may be further improved with the use of suitable electrolytes.

4.4 Other applications

MXene has also been explored in other energy storage devices. For example, Liang *et al.* reported that MXene sheets are excellent sulfur hosts for Li-S batteries [63], and Wang *et al.* demonstrated that MXene nanosheets are promising electrode materials for Na-ion hybrid capacitors [64]. These research directions deserve extended future investigations.

In fields other than electrochemistry, MXenes' unique structures and properties provide the material class with many other potential applications, including adsorbents [16, 65], hydrogen storage media [66, 67], catalyst supporters [21, 68, 69], additives [70, 71], and many others [72–75]. However, many of these applications are still hypothetical or at the fundamental stage. Future investigations are necessary to confirm the applicability of MXenes to these fields, and we will briefly discuss possible research directions in this section.

Its large and highly accessible hydrophilic surfaces provide MXene with good adsorption performance, permitting its possible use in adsorbents, similar to other layered materials. Peng *et al.* prepared an alk-MXene ($Ti_3C_2(OH/ONa)_xF_{2-x}$) by the alkalization intercalation of exfoliated MXene [65]. This alk-MXene displayed excellent Pb(II) adsorption performances, with effluent contents below 2 μg/L. Intriguingly, the exhausted materials can be efficiently regenerated, with desorbed Pb(II) efficiencies up to 95.2%. Mashtalir *et al.* studied the adsorption of dyes on $Ti_3C_2T_x$ [16]. Although the adsorption capacities were smaller than the observed values typical of commercial activated carbons, more modifications may improve the adsorption performance, which should be explored in the future.

Transition metals are strong candidates for improving the binding energy of hydrogen on sorption-based hydrogen storage materials, due to the Kubas interaction. Hu *et al.* computationally investigated the possibility of using Ti_2C as a hydrogen storage medium, as all transition metals are located in the surface in unsaturated coordination states [66]. The results showed that hydrogen can be adsorbed on both sides of Ti_2C, with a calculated maximum capacity of 8.6 wt.%, exceeding the target value of 5.5 wt.%. The hydrogen storage performance of Sc_2C was also studied computationally [67]. The result (9.0 wt.%) exceeded even that of Ti_2C. Therefore, MXenes may be fascinating materials for hydrogen storage, pending experimental confirmation.

MXenes' 2D nature and large surface areas also favors the materials for applications as supports or carriers. Li *et al.* applied $Ti_3C_2T_2$ as a carrier for depositing Ru nanoparticles ($Ru/Ti_3C_2T_2$) [68]. The prepared nanocomposite exhibited excellent catalytic activity for hydrogen generation via the room-temperature hydrolysis of $NaBH_4$. The reported hydrogen generation rate was 59.04 L H_2/g_{Ru}·min, exceeding those of other additive-free Ru-based catalysts at comparable reaction temperatures. However, the aggregation of metal particles and the poisoning of active sites by BO^{2-} generated during hydrolysis remain as challenges to be solved. Further improvements are necessary for the practical application.

Another nanocomposite, MXene-Cu_2O, demonstrated

a higher catalytic activity compared with either MXene or Cu_2O separately for thermally decomposing ammonium perchlorate (AP) [69]. This enhanced activity was ascribed to several reasons, including the increased surface areas of Cu_2O in the presence of MXene, improved heat transfer due to the good thermal conductivity of MXene, and the decomposition of reactant molecules adsorbed on the surface of MXene layers, which accelerated the decomposition of AP.

MXene species are also potential additives. Yang *et al.* tested the feasibility of using $Ti_3C_2T_x$ as a lubrication additive in base oils [70]. Layered $Ti_3C_2T_x$ could greatly enhance the friction-reduction and anti-friction properties of base oils, especially under high applied loads. Under high applied loads, $Ti_3C_2T_x$ may form a uniform lubricant film, which not only has good lubricating effects, but also avoids direct contact between mechanical counterparts. Thus, MXenes could potentially be good candidates as lubricating materials.

5 Summary and outlook

Studies on graphene have generated great enthusiasm in the exploration of 2D materials. Among these materials, MXene, exfoliated from layered MAX phases, has received growing interest in recent years. The distinctive properties of MXene sheets make them promising candidates as alternatives to graphene. This review summarizes the latest progress in computational and experimental studies of MXene and reflects the rapid development of the MXene research community. The advances achieved in preparation and properties, together with the explored applications of MXene, provide a strong impetus to further progress in the characterization and use of these new 2D materials.

Compared with the intensive studies on graphene, investigations on MXene are still in embryonic stages. Many opportunities and challenges exist simultaneously. These include the preparation of bare MXenes; the exfoliation of new MXenes; the studies on their 1D forms [76, 77]; the practical measurements of their magnetic, elastic, and optical properties; and their potential applications. All await further research efforts and increased understanding. We are convinced that this new class of 2D materials has good potential, and we hope more researchers will explore this area of materials and produce significant scientific developments.

Acknowledgements This work was supported by the National Natural Science Foundation of China (Grant No. 21273118), National Fund for Fostering Talents of Basic Science (Grant No. J1103306), and Innovation Team of Ministry of Education (IRT13022) in China.

References

1. K. S. Novoselov, A. K. Geim, S. V. Morozov, D. Jiang, Y. Zhang, S. V. Dubonos, I. V. Grigorieva, and A. A. Firsov, Electric field effect in atomically thin carbon films, *Science* 306(5696), 666 (2004)
2. A. K. Geim and K. S. Novoselov, The rise of graphene, *Nat. Mater.* 6(3), 183 (2007)
3. S. Guo and S. Dong, Graphene nanosheet: Synthesis, molecular engineering, thin film, hybrids, and energy and analytical applications, *Chem. Soc. Rev.* 40(5), 2644 (2011)
4. V. Singh, D. Joung, L. Zhai, S. Das, S. I. Khondaker, and S. Seal, Graphene based materials: Past, present and future, *Prog. Mater. Sci.* 56(8), 1178 (2011)
5. T. Kuila, S. Bose, A. K. Mishra, P. Khanra, N. H. Kim, and J. H. Lee, Chemical functionalization of graphene and its applications, *Prog. Mater. Sci.* 57(7), 1061 (2012)
6. Q. Tang, Z. Zhou, and Z. Chen, Graphene-related nanomaterials: Tuning properties by functionalization, *Nanoscale* 5(11), 4541 (2013)
7. Q. Tang and Z. Zhou, Graphene-analogous low-dimensional materials, *Prog. Mater. Sci.* 58(8), 1244 (2013)
8. M. Naguib and Y. Gogotsi, Synthesis of two-dimensional materials by selective extraction, *Acc. Chem. Res.* 48(1), 128 (2015)
9. Y. Jing, Z. Zhou, C. R. Cabrera, and Z. Chen, Graphene, inorganic graphene analogs and their composites for lithium ion batteries, *J. Mater. Chem. A* 2(31), 12104 (2014)
10. M. Naguib, M. Kurtoglu, V. Presser, J. Lu, J. Niu, M. Heon, L. Hultman, Y. Gogotsi, and M. W. Barsoum, Two-dimensional nanocrystals produced by exfoliation of Ti_3AlC_2, *Adv. Mater.* 23(37), 4248 (2011)
11. I. R. Shein and A. L. Ivanovskii, Graphene-like nanocarbides and nanonitrides of d metals (MXenes): synthesis, properties and simulation, *Micro & Nano Lett.* 8(2), 59 (2013)
12. M. W. Barsoum and M. A. X. Phases, Properties of Machinable Ternary Carbides and Nitrides, Wiley & Sons, 2013
13. M. Naguib, O. Mashtalir, J. Carle, V. Presser, J. Lu, L. Hultman, Y. Gogotsi, and M. W. Barsoum, Two-dimensional transition metal carbides, *ACS Nano* 6(2), 1322 (2012)
14. M. Naguib, J. Halim, J. Lu, K. M. Cook, L. Hultman, Y. Gogotsi, and M. W. Barsoum, New two-dimensional niobium and vanadium carbides as promising materials for li-ion batteries, *J. Am. Chem. Soc.* 135(43), 15966 (2013)
15. M. Ghidiu, M. Naguib, C. Shi, O. Mashtalir, L. M. Pan, B. Zhang, J. Yang, Y. Gogotsi, S. J. L. Billinge, and M. W. Barsoum, Synthesis and characterization of two-dimensional Nb_4C_3 (MXene), *Chem. Commun.* 50(67), 9517 (2014)
16. O. Mashtalir, K. M. Cook, V. N. Mochalin, M. Crowe, M. W. Barsoum, and Y. Gogotsi, Dye adsorption and decomposi-

tion on two-dimensional titanium carbide in aqueous media, *J. Mater. Chem. A* 2(35), 14334 (2014)

17. M. Kurtoglu, M. Naguib, Y. Gogotsi, and M. W. Barsoum, First principles study of two-dimensional early transition metal carbides, *MRS Commun.* 2(04), 133 (2012)
18. M. Khazaei, M. Arai, T. Sasaki, C. Y. Chung, N. S. Venkataramanan, M. Estili, Y. Sakka, and Y. Kawazoe, Novel electronic and magnetic properties of two-dimensional transition metal carbides and nitrides, *Adv. Funct. Mater.* 23(17), 2185 (2013)
19. J. Come, M. Naguib, P. Rozier, M. W. Barsoum, Y. Gogotsi, P. L. Taberna, M. Morcrette, and P. Simon, A non-aqueous asymmetric cell with a Ti_2C-based two-dimensional negative electrode, *J. Electrochem. Soc.* 159(8), A1368 (2012)
20. J. Hu, B. Xu, C. Ouyang, S. A. Yang, and Y. Yao, Investigations on V_2C and V_2CX_2 (X = F, OH) monolayer as a promising anode material for li ion batteries from first-principles calculations, *J. Phys. Chem. C* 118(42), 24274 (2014)
21. X. Xie, S. Chen, W. Ding, Y. Nie, and Z. Wei, An extraordinarily stable catalyst: Pt NPs supported on two-dimensional $Ti_3C_2X_2$ (X = OH, F) nanosheets for oxygen reduction reaction, *Chem. Commun.* 49(86), 10112 (2013)
22. F. Wang, C. H. Yang, C. Y. Duan, D. Xiao, Y. Tang, and J. F. Zhu, An organ-like titanium carbide material (MXene) with multilayer structure encapsulating hemoglobin for a mediator-free biosensor, *J. Electrochem. Soc.* 162(1), B16 (2015)
23. M. Naguib, V. N. Mochalin, M. W. Barsoum, and Y. Gogotsi, 25th anniversary article: MXenes: A new family of two-dimensional materials, *Adv. Mater.* 26(7), 992 (2014)
24. O. Mashtalir, M. Naguib, V. N. Mochalin, Y. Dall'Agnese, M. Heon, M. W. Barsoum, and Y. Gogotsi, Intercalation and delamination of layered carbides and carbonitrides, *Nat. Commun.* 4, 1716 (2013)
25. F. Chang, C. Li, J. Yang, H. Tang, and M. Xue, Synthesis of a new graphene-like transition metal carbide by de-intercalating Ti_3AlC_2, *Mater. Lett.* 109, 295 (2013)
26. J. Halim, M. R. Lukatskaya, K. M. Cook, J. Lu, C. R. Smith, L. A. Naslund, S. J. May, L. Hultman, Y. Gogotsi, P. Eklund, and M. W. Barsoum, Transparent conductive two-dimensional titanium carbide epitaxial thin films, *Chem. Mater.* 26(7), 2374 (2014)
27. M. Ghidiu, M. R. Lukatskaya, M. Q. Zhao, Y. Gogotsi, and M. W. Barsoum, Conductive two-dimensional titanium carbide 'clay' with high volumetric capacitance, *Nature* 516(7529), 78 (2014)
28. O. Mashtalir, M. Naguib, B. Dyatkin, Y. Gogotsi, and M. W. Barsoum, Kinetics of aluminum extraction from Ti_3AlC_2 in hydrofluoric acid, *Mater. Chem. Phys.* 139(1), 147 (2013)
29. Y. Xie, M. Naguib, V. N. Mochalin, M. W. Barsoum, Y. Gogotsi, X. Q. Yu, K. W. Nam, X. Q. Yang, A. I. Kolesnikov, and P. R. C. Kent, Role of surface structure on li-ion energy storage capacity of two-dimensional transition-metal carbides, *J. Am. Chem. Soc.* 136(17), 6385 (2014)
30. Y. Xie, Y. Dall'Agnese, M. Naguib, Y. Gogotsi, M. W. Barsoum, H. L. L. Zhuang, and P. R. C. Kent, Prediction and characterization of MXene nanosheet anodes for non-lithium-ion batteries, *ACS Nano* 8(9), 9606 (2014)
31. T. Hu, J. Wang, H. Zhang, Z. Li, M. Hu, and X. Wang, Vibrational properties of Ti_3C_2 and $Ti_3C_2T_2$ (T = O, F, OH) monosheets by first-principles calculations: A comparative study, *Phys. Chem. Chem. Phys.* 17(15), 9997 (2015)
32. Q. Tang, Z. Zhou, and P. W. Shen, Are MXenes promising anode materials for Li ion batteries? Computational studies on electronic properties and Li storage capability of Ti_3C_2 and $Ti_3C_2X_2$ (X = F, OH) monolayer, *J. Am. Chem. Soc.* 134(40), 16909 (2012)
33. X. Wang, X. Shen, Y. Gao, Z. Wang, R. Yu, and L. Chen, Atomic-scale recognition of surface structure and intercalation mechanism of Ti_3C_2X, *J. Am. Chem. Soc.* 137(7), 2715 (2015)
34. A. N. Enyashin and A. L. Ivanovskii, Two-dimensional titanium carbonitrides and their hydroxylated derivatives: Structural, electronic properties and stability of MXenes $Ti_3C_{2tx}N_x(OH)_2$ from DFTB calculations, *J. Solid State Chem.* 207, 42 (2013)
35. V. Mauchamp, M. Bugnet, E. P. Bellido, G. A. Botton, P. Moreau, D. Magne, M. Naguib, T. Cabioc'h, and M. W. Barsoum, Enhanced and tunable surface plasmons in two-dimensional Ti_3C_2 stacks: Electronic structure versus boundary effects, *Phys. Rev. B* 89(23), 235428 (2014)
36. I. R. Shein and A. L. Ivanovskii, Planar nano-block structures $Ti_{n+1}Al_{0.5}C_n$ and $Ti_{n+1}C_n$ (n=1, and 2) from MAX phases: Structural, electronic properties and relative stability from first principles calculations, *Superlattices Microstruct.* 52(2), 147 (2012)
37. I. R. Shein and A. L. Ivanovskii, Graphene-like titanium carbides and nitrides $Ti_{n+1}C_n$, $Ti_{n+1}N_n$ (n=1, 2, and 3) from de-intercalated MAX phases: First-principles probing of their structural, electronic properties and relative stability, *Comput. Mater. Sci.* 65, 104 (2012)
38. Y. Xie and P. R. C. Kent, Hybrid density functional study of structural and electronic properties of functionalized $Ti_{n+1}X_n$ (X = C, N) monolayers, *Phys. Rev. B* 87(23), 235441 (2013)
39. S. Zhao, W. Kang, and J. Xue, Manipulation of electronic and magnetic properties of M_2C (M = Hf, Nb, Sc, Ta, Ti, V, Zr) monolayer by applying mechanical strains, *Appl. Phys. Lett.* 104(13), 133106 (2014)
40. S. Wang, J. X. Li, Y. L. Du, and C. Cui, First-principles study on structural, electronic and elastic properties of graphene-like hexagonal Ti_2C monolayer, *Comput. Mater. Sci.* 83, 290 (2014)
41. M. Khazaei, M. Arai, T. Sasaki, M. Estili, and Y. Sakka, Two-dimensional molybdenum carbides: Potential thermo-

electric materials of the MXene family, *Phys. Chem. Chem. Phys.* 16(17), 7841 (2014)

42. H. Lashgari, M. R. Abolhassani, A. Boochani, S. M. Elahi, and J. Khodadadi, Electronic and optical properties of 2D graphene-like compounds titanium carbides and nitrides: DFT calculations, *Solid State Commun.* 195, 61 (2014)
43. A. N. Enyashin and A. L. Ivanovskii, Structural and electronic properties and stability of MXenes Ti_2C and Ti_3C_2 functionalized by Methoxy groups, *J. Phys. Chem. C* 117(26), 13637 (2013)
44. Y. Lee, S. B. Cho, and Y. C. Chung, Tunable indirect to direct band gap transition of monolayer Sc_2CO_2 by the strain effect, *ACS Appl. Mater. Interfaces* 6(16), 14724 (2014)
45. Y. Lee, Y. Hwang, S. B. Cho, and Y. C. Chung, Achieving a direct band gap in oxygen functionalized-monolayer scandium carbide by applying an electric field, *Phys. Chem. Chem. Phys.* 16(47), 26273 (2014)
46. N. J. Lane, M. W. Barsoum, and J. M. Rondinelli, Correlation effects and spin-orbit interactions in two-dimensional hexagonal 5d transition metal carbides, $Ta_{n+1}C_n$ (n = 1,2,3), *EPL* 101(5), 57004 (2013)
47. M. Naguib, O. Mashtalir, M. R. Lukatskaya, B. Dyatkin, C. Zhang, V. Presser, Y. Gogotsi, and M. W. Barsoum, One-step synthesis of nanocrystalline transition metal oxides on thin sheets of disordered graphitic carbon by oxidation of MXenes, *Chem. Commun.* 50(56), 7420 (2014)
48. H. Ghassemi, W. Harlow, O. Mashtalir, M. Beidaghi, M. R. Lukatskaya, Y. Gogotsi, and M. L. Taheri, In situ environmental transmission electron microscopy study of oxidation of two-dimensional Ti_3C_2 and formation of carbon-supported TiO_2, *J. Mater. Chem. A Mater. Energy Sustain.* 2(35), 14339 (2014)
49. Z. Y. Li, L. B. Wang, D. D. Sun, Y. D. Zhang, B. Z. Liu, Q. K. Hu, and A. G. Zhou, Synthesis and thermal stability of two-dimensional carbide MXene Ti_3C_2, *Mater. Sci. Eng. B* 191, 33 (2015)
50. J. X. Li, Y. L. Du, C. X. Huo, S. Wang, and C. Cui, Thermal stability of two-dimensional Ti_2C nanosheets, *Ceram. Int.* 41(2), 2631 (2015)
51. M. Naguib, J. Come, B. Dyatkin, V. Presser, P. L. Taberna, P. Simon, M. W. Barsoum, and Y. Gogotsi, MXene: A promising transition metal carbide anode for lithium-ion batteries, *Electrochem. Commun.* 16(1), 61 (2012)
52. C. Eames and M. S. Islam, Ion intercalation into two-dimensional transition-metal carbides: Global screening for new high-capacity battery materials, *J. Am. Chem. Soc.* 136(46), 16270 (2014)
53. D. D. Sun, M. S. Wang, Z. Y. Li, G. X. Fan, L. Z. Fan, and A. G. Zhou, Two-dimensional Ti_3C_2 as anode material for Li-ion batteries, *Electrochem. Commun.* 47, 80 (2014)
54. M. D. Levi, M. R. Lukatskaya, S. Sigalov, M. Beidaghi, N. Shpigel, L. Daikhin, D. Aurbach, M. W. Barsoum, and Y. Gogotsi, *Adv. Energy Mater.* 5, 1400815 (2014)
55. S. J. Zhao, W. Kang, and J. M. Xue, Role of strain and concentration on the li adsorption and diffusion properties on Ti_2C layer, *J. Phys. Chem. C* 118(27), 14983 (2014)
56. J. B. Goodenough and K. S. Park, The Li-ion rechargeable battery: A perspective, *J. Am. Chem. Soc.* 135(4), 1167 (2013)
57. D. Q. Er, J. W. Li, M. Naguib, Y. Gogotsi, and V. B. Shenoy, Ti_3C_2 MXene as a high capacity electrode material for metal (Li, Na, K, Ca) ion batteries, *ACS Appl. Mater. Interfaces* 6(14), 11173 (2014)
58. M. R. Lukatskaya, O. Mashtalir, C. E. Ren, Y. Dall'Agnese, P. Rozier, P. L. Taberna, M. Naguib, P. Simon, M. W. Barsoum, and Y. Gogotsi, Cation intercalation and high volumetric capacitance of two-dimensional titanium carbide, *Science* 341(6153), 1502 (2013)
59. E. Yang, H. Ji, J. Kim, H. Kim, and Y. Jung, Exploring the possibilities of two-dimensional transition metal carbides as anode materials for sodium batteries, *Phys. Chem. Chem. Phys.* 17(7), 5000 (2015)
60. Y. Dall'Agnese, M. R. Lukatskaya, K. M. Cook, P. L. Taberna, Y. Gogotsi, and P. Simon, High capacitance of surface-modified 2D titanium carbide in acidic electrolyte, *Electrochem. Commun.* 48, 118 (2014)
61. Z. Ling, C. E. Ren, M. Q. Zhao, J. Yang, J. M. Giammarco, J. S. Qiu, M. W. Barsoum, and Y. Gogotsi, Flexible and conductive MXene films and nanocomposites with high capacitance, *Proc. Natl. Acad. Sci. USA* 111(47), 16676 (2014)
62. M. Q. Zhao, C. E. Ren, Z. Ling, M. R. Lukatskaya, C. Zhang, K. L. Van Aken, M. W. Barsoum, and Y. Gogotsi, Flexible MXene/carbon nanotube composite paper with high volumetric capacitance, *Adv. Mater.* 27(2), 339 (2015)
63. X. Liang, A. Garsuch, and L. F. Nazar, Sulfur cathodes based on conductive MXene nanosheets for high-performance lithium-sulfur batteries, *Angew. Chem. Int. Ed.* 54(13), 3907 (2015)
64. X. Wang, S. Kajiyama, H. Iinuma, E. Hosono, S. Oro, I. Moriguchi, M. Okubo, and A. Yamada, Pseudocapacitance of MXene nanosheets for high-power sodium-ion hybrid capacitors, *Nat. Commun.* 6, 6544 (2015)
65. Q. M. Peng, J. X. Guo, Q. R. Zhang, J. Y. Xiang, B. Z. Liu, A. G. Zhou, R. P. Liu, and Y. J. Tian, Unique lead adsorption behavior of activated hydroxyl group in two-dimensional titanium carbide, *J. Am. Chem. Soc.* 136(11), 4113 (2014)
66. Q. K. Hu, D. D. Sun, Q. H. Wu, H. Y. Wang, L. B. Wang, B. Z. Liu, A. G. Zhou, and J. L. He, MXene: A new family of promising hydrogen storage medium, *J. Phys. Chem. A* 117(51), 14253 (2013)
67. Q. K. Hu, H. Y. Wang, Q. H. Wu, X. T. Ye, A. G. Zhou, D. D. Sun, L. B. Wang, B. Z. Liu, and J. L. He, Two-dimensional Sc_2C: A reversible and high-capacity hydrogen storage material predicted by first-principles calculations, *Int. J. Hydrogen Energy* 39(20), 10606 (2014)
68. X. Li, G. Fan, and C. Zeng, Synthesis of ruthenium nanoparticles deposited on graphene-like transition metal carbide as

an effective catalyst for the hydrolysis of sodium borohydride, *Int. J. Hydrogen Energy* 39(27), 14927 (2014)

69. Y. P. Gao, L. B. Wang, Z. Y. Li, A. G. Zhou, Q. K. Hu, and X. X. Cao, Preparation of MXene-Cu_2O nanocomposite and effect on thermal decomposition of ammonium perchlorate, *Solid State Sci.* 35, 62 (2014)
70. J. Yang, B. Chen, H. Song, H. Tang, and C. Li, Synthesis, characterization, and tribological properties of two-dimensional Ti_3C_2, *Cryst. Res. Technol.* 49(11), 926 (2014)
71. X. H. Zhang, M. Q. Xue, X. H. Yang, Z. P. Wang, G. S. Luo, Z. D. Huang, X. L. Sui, and C. S. Li, Preparation and tribological properties of $Ti_3C_2(OH)_2$ nanosheets as additives in base oil, *RSC Adv.* 5(4), 2762 (2015)
72. Z. N. Ma, Z. P. Hu, X. D. Zhao, Q. Tang, D. H. Wu, Z. Zhou, and L. X. Zhang, Tunable band structures of heterostructured bilayers with transition-metal dichalcogenide and MXene monolayer, *J. Phys. Chem. C* 118(10), 5593 (2014)
73. J. Chen, K. Chen, D. Tong, Y. Huang, J. Zhang, J. Xue, Q. Huang, and T. Chen, CO_2 and temperature dual responsive "Smart" MXene phases, *Chem. Commun.* 51(2), 314 (2015)
74. Y. Lee, Y. Hwang, and Y. C. Chung, Achieving type I, II, and III heterojunctions using functionalized MXene, *ACS Appl. Mater. Interfaces* 7(13), 7163 (2015)
75. X. Li, Y. Dai, Y. Ma, Q. Liu, and B. Huang, Intriguing electronic properties of two-dimensional MoS_2 /TM_2CO_2 (TM = Ti, Zr, or Hf) hetero-bilayers: Type-II semiconductors with tunable band gaps, *Nanotechnology* 26(13), 135703 (2015)
76. X. Zhang, Z. Ma, X. Zhao, Q. Tang, and Z. Zhou, Computational studies on structural and electronic properties of functionalized MXene monolayers and nanotubes, *J. Mater. Chem. A* 3(9), 4960 (2015)
77. S. J. Zhao, W. Kang, and J. M. Xue, MXene nanoribbons, *J. Mater. Chem. C* 3(4), 879 (2015)